Design and Performance of Microwave Amplifiers with GaAs Schottky-Gate Field-Effect Transistors

CHARLES A. LIECHTI, MEMBER, IEEE, AND ROBERT L. TILLMAN

***Abstract*—The design and performance of an X-band amplifier with GaAs Schottky-gate field-effect transistors are described. The amplifier achieves 20 ± 1.3-dB gain with a 5.5-dB typical noise figure (6.9 dB maximum) over the frequency range of 8.0–12.0 GHz. The VSWR at the input and output ports does not exceed 2.5:1. The minimum output power for 1-dB gain compression is +13 dBm, and the intercept point for third-order intermodulation products is +26 dBm. The design of practical wide-band coupling networks is discussed. These networks minimize the overall amplifier noise figure and maintain a constant gain in the band.**

I. INTRODUCTION

IT HAS BEEN demonstrated that GaAs field-effect transistors with Schottky-barrier gates (MESFET's) combine low-noise properties with high gain and large dynamic range in a frequency range that has not been invaded by bipolar transistors [1]–[3]. Recent advances in GaAs materials and device technology have made possible the fabrication of reliable MESFET's with 0.2-μm channels and 1-μm gate structures with reasonable yield and in satisfactory quantities.

Several successful microwave FET amplifier designs have been reported [3]–[10]. Some have proven that very wide band amplification is feasible with these devices in X and Ku bands [9], [10]. These designs are based on empirical network topologies (except [10]), and the circuit elements have been computer optimized for maximum gain. This paper describes networks that are especially suitable for coupling power in and out of microwave FET's. The choice of the particular circuit topology is justified and performance limits are outlined. A step-by-step procedure for designing an amplifier with minimum noise figure and constant gain will be described. This design is based on established matching network theory and requires the use of a computer only for very broad bandwidths. The experimental results prove that high-gain and low-noise figures can be simultaneously achieved over a band as wide as 8–12 GHz.

The topics are treated in the following sequence. First, the transistor properties relevant to the circuit design are described. Second, the principles and procedures for the network synthesis are presented, and the basic amplifier construction is outlined. Third, the experimental results from an X-band amplifier are discussed leading to the final conclusions.

Manuscript received August 21, 1973; revised December 6, 1973. This work was supported jointly by Hewlett-Packard Company and the U. S. Army Electronics Command, Fort Monmouth, N. J., under Contract DAAB07-72-C-0322.

C. A. Liechti is with the Solid-State Laboratory, Hewlett-Packard Company, Palo Alto, Calif. 94304.

R. L. Tillman was with the Solid-State Laboratory, Hewlett-Packard Company, Palo Alto, Calif. 94304. He is now with the Microwave Technology Center, Hewlett-Packard Company, Palo Alto, Calif. 94304.

II. MESFET CHARACTERISTICS

The MESFET structure is illustrated in the scanning electron micrograph of Fig. 1. The dc current flows from drain to source in an 0.2-μm-thin epitaxial layer, doped with 1×10^{17} donors/cm^3, and grown on a semi-insulating GaAs substrate. The current is controlled by the depth of a depletion layer that extends beneath the Schottky-barrier gate. The gate is a 1-μm-wide and 500-μm-long metal stripe. Source and drain are alloyed Au–Ge ohmic contacts. They are separated from the gate by 1 and 2 μm, respectively. Outside the active device area, the epitaxial film is removed by mesa etching. This permits a large gate contact pad to be located on the semiinsulating substrate where it contributes only a small fraction to the overall gate to source capacitance. The drain and gate are contacted with an overlay metallization which runs over the mesa step. The transistor chip has a size of 0.010 × 0.025 in. The chips are tested from dc through 13 GHz in a fixture that makes pressure contact to the overlay metallization with negligible parasitic reactances [2].

The noise figure F_a of an amplifier which consists of a large number of cascaded identical stages with gain G and noise figure F is

$$F_a = 1 + \frac{F - 1}{1 - 1/G} = 1 + M \qquad (1)$$

where M is the noise measure. In order to minimize the amplifier noise figure, it is necessary to minimize the noise measure rather than the noise figure of each stage. This distinction is essential in finding the optimum dc bias of the transistor. With 4-V drain voltage, the MESFET in this example exhibits maximum gain at 80 mA, minimum noise measure at 30 mA, and minimum noise figure at 17-mA drain current. At $I_{DS} = 30$ mA, the source admittance has been optimized, first, for minimum noise figure, second, for minimum noise measure, and third, for maximum gain [11]. The associated noise figures and gains are plotted in Fig. 2. Since the MESFET exhibits high gain in this frequency range, the source admittances for minimum noise measure and noise figure are nearly identical. The noise figure increases from 3.3 dB at 8 GHz

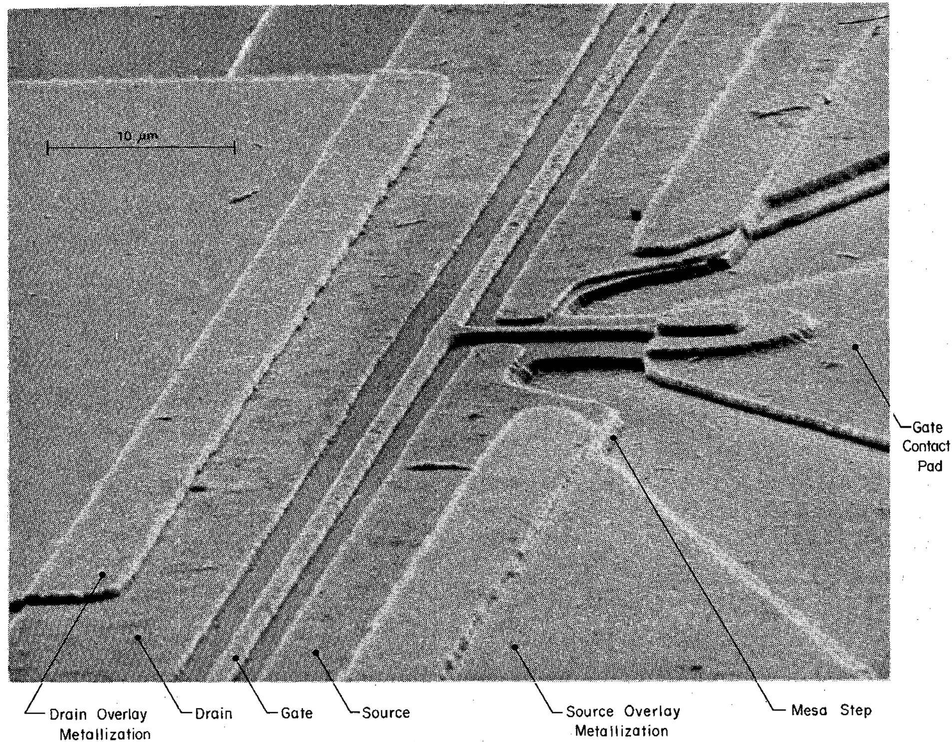

Fig. 1. Scanning electron micrograph of the MESFET's center section.

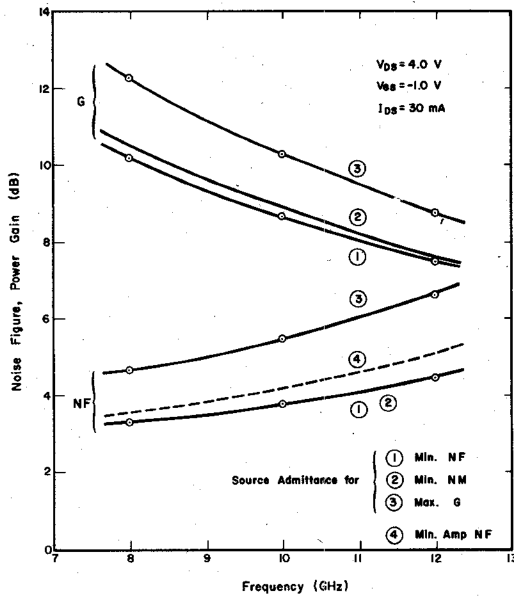

Fig. 2. MESFET power gain and noise figure versus frequency for source admittances that yield minimum noise figure ①, minimum noise measure ②, and maximum gain ③. Curve ④ shows the minimum noise figure for a large number of identical cascaded stages.

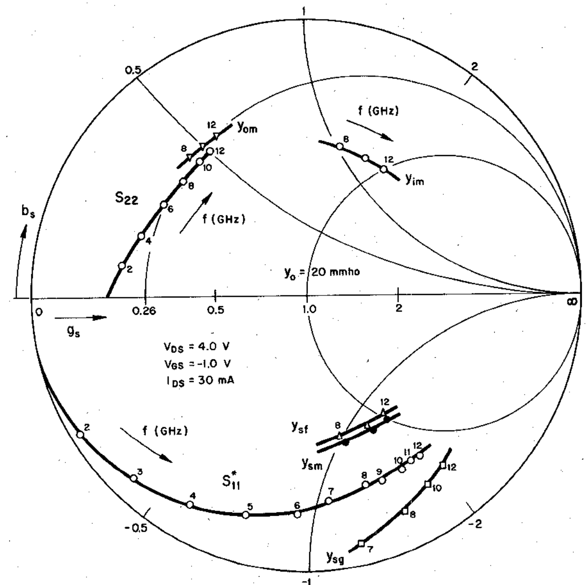

Fig. 3. Optimum source admittance that yields minimum noise figure Y_{sf}, minimum noise measure Y_{sm}, and maximum gain Y_{sg}. Also plotted are the MESFET scattering parameters s_{11}^*, s_{22}, the MESFET's output admittance Y_{om}, for an input noise measure match, and the equivalent noise input admittance $Y_{im} = Y_{sm}^*$.

to 4.5 dB at 12 GHz, and the associated gain (curve ②) drops with a 4.7-dB/octave slope from 10.4 to 7.6 dB. With these data, the lowest possible total amplifier noise figure can be predicted from (1). It is shown in curve ④.

The optimum source admittances referenced to the input plane of the MESFET chip are shown in the Smith chart of Fig. 3 with frequency as a parameter. Y_{sf} applies to the case of minimum noise figure, Y_{sm} to minimum noise measure, and Y_{sg} to maximum gain. For comparison, the complex conjugate of the scattering parameter s_{11} is also plotted. Y_{sg} and Y_{sm} and the associated noise figures are substantially different. Consequently, the conventional circuit optimization on the basis of MESFET s parameters is not adequate for a low-noise amplifier design.

The output scattering parameter s_{22} is shown in the upper half of the Smith chart. For a noise measure match

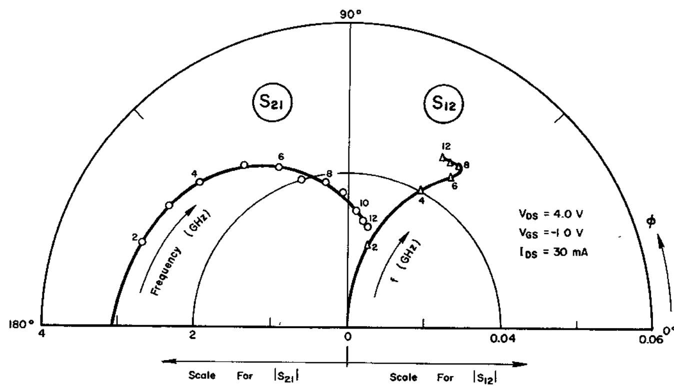

Fig. 4. MESFET scattering parameters s_{12} and s_{21} versus frequency.

at the input (source admittance Y_{sm}), the MESFET's output admittance Y_{om} lies on a constant conductance circle with increasing capacitive susceptance for increasing frequency. In a limited band around 10 GHz, the output admittance can be modeled as a resistor, $R_{om} = 192\ \Omega$, in parallel with a capacitor, $C_{om} = 0.16$ pF. In order to provide the complete set of s parameters, s_{12} and s_{21} are plotted versus frequency in Fig. 4.

For frequencies sufficiently above the instability limit (6.5 GHz), the MESFET can approximately be treated as a unilateral device. This is demonstrated in Fig. 3 with the proximity of Y_{sg} to s_{11}^* and Y_{om} to s_{22}. The unilateral assumption breaks the MESFET equivalent circuit into two decoupled networks, a series RC at the input, and a parallel RC at the output. This approximation is utilized in the design techniques of Section III.

III. AMPLIFIER DESIGN

A. Input Matching Network

For receiver preamplifiers, the design objective is minimum amplifier noise figure rather than maximum gain. The main task is to synthesize the optimum source admittance Y_{sm} for minimum transistor noise measure at the FET input plane. An approximate solution can be found in the following way. An equivalent noise input admittance Y_{im} is defined as the complex conjugate of Y_{sm}. The two admittances are plotted in Fig. 3 versus frequency. Y_{im} can be approximated with a capacitance C_{im} in series with a resistance R_{im} with good accuracy over an octave bandwidth. The values, $C_{im} = 0.57$ pF and $R_{im} = 21\ \Omega$, are determined in Fig. 3.[1] The task consists of designing a Chebyshev impedance-matching network to match the generator admittance Y_0 to the noise input admittance Y_{im}. Chebyshev prototypes are selected to maximize the bandwidth and provide a good match at the band edges.

The first step is to establish the number of resonators required to synthesize Y_{sm} with a specified accuracy between the lower and upper band edges, f_l and f_u. The accuracy limits are determined by the tolerated excess noise figure. The minimum source admittance deviation from Y_{sm} which causes a maximum noise figure increase of 0.5 dB between 8 and 12 GHz has been determined.[2] This admittance deviation can be expressed in terms of a maximum tolerated VSWR. The computation yields 1.3:1. In synthesizing Y_{sm} with a Chebyshev impedance-matching network, the bandwidth can be computed using the VSWR versus load decrement curves plotted in [12, fig. 4.09-3]. The result is illustrated in Fig. 5 showing the maximum theoretical bandwidth w versus center frequency f_0 with the number of resonators n as a parameter. The curves are computed for a load with $C_{im} = 0.57$ pF in series with $R_{im} = 21\ \Omega$. A single resonator structure ($n = 1$) consisting of a series inductance and an impedance inverter (transformer) has an 8.9–11.1-GHz bandwidth. A more complex circuit with two additional resonators ($n = 3$) extends the band from 6 to 14 GHz.

The network shown in Fig. 6 was found to provide wide-band impedance matching, amplifier stability, and easy realization. The MESFET's equivalent noise input admittance is resonated with the series inductance L_1 and coupled to a network consisting of two $\lambda/4$ resonators. The resistance R_{im} can be considered the load resistance and $L_1 - C_{im}$ the last resonator of a three-stage bandpass filter coupling R_{im} to the source resistance Z_0. All resonators are resonant at the band center frequency f_0 and are coupled alternately by impedance inverters and admittance inverters. The inverters perform two functions. They convert the circuit connected to their output into its dual form at their input. This property allows the use of only one kind of resonator (e.g., series circuits). In addition, the inverters act as impedance transformers. This enables the designer to choose the characteristic impedance of the $\lambda/4$ resonators and adjust the inverter constants, K_{12}, J_{23}, and K_{34}, to ensure that the resonator reactance slopes at f_0 and the source resistance have the relationship prescribed by the Chebyshev impedance-matching prototype. If the line impedances are chosen to be equal to the source impedance Z_0 then the inverter constants are [12]

$$K_{12} = Z_0 \left(\frac{\pi w}{4 g_1 g_2} \frac{R_{im}}{Z_0 \delta} \right)^{1/2} \tag{2}$$

$$J_{23} = \frac{1}{Z_0} \frac{\pi w}{4} \left(\frac{1}{g_2 g_3} \right)^{1/2} \tag{3}$$

$$K_{34} = Z_0 \left(\frac{\pi w}{4 g_3 g_4} \right)^{1/2} \tag{4}$$

where w is the relative bandwidth:

$$w = (f_u - f_l)/f_0 \tag{5}$$

[1] The actual MESFET input admittance, $Y_{ig} = Y_{sg}^*$, with $C_{ig} = 0.58$ pF in series with $R_{ig} = 7\ \Omega$ has a considerably smaller series resistance than Y_{im}.

[2] The direction and magnitude of the worst admittance deviation are found graphically by plotting the constant noise figure contours in the source admittance plane at various frequencies [11]. The four noise parameters, required for this plot, are determined from data given in Figs. 2 and 3.

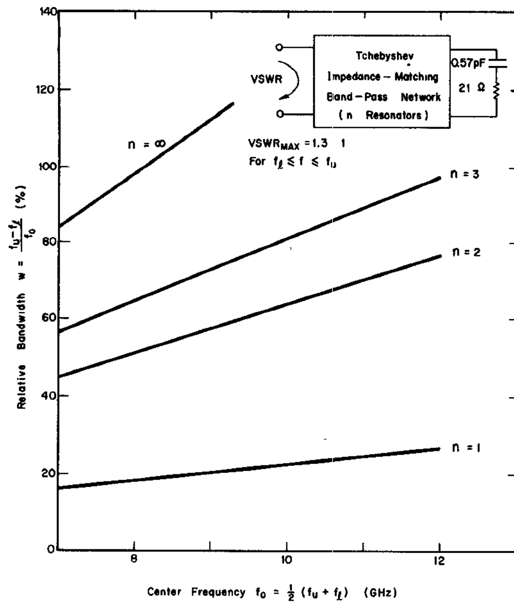

Fig. 5. Maximum bandwidth w versus center frequency f_0 for Chebyshev impedance-matching networks with n resonators.

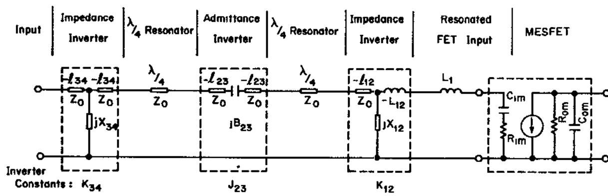

Fig. 6. MESFET with input matching network.

f_0 the center frequency:

$$f_0 = \tfrac{1}{2}(f_u + f_l) \tag{6}$$

δ the decrement of the load impedance at f_0:

$$\delta = (2\pi f_0 R_{im} C_{im})/w \tag{7}$$

and g_1, g_2, g_3, and g_4 the normalized element values of the Chebyshev impedance-matching prototype for the decrement δ [12].

The elements shown in the circuit diagram of Fig. 6 can now be computed using the following formulas [12].

1) Series Inductance:

$$L_1 = \frac{1}{(2\pi f_0)^2 C_{im}}. \tag{8}$$

2) Impedance Inverters:

$$X_{ik} = \frac{K_{ik}}{1 - (K_{ik}/Z_0)^2} \tag{9}$$

$$l_{ik} = \frac{\lambda}{4\pi} \tan^{-1}\left(\frac{2X_{ik}}{Z_0}\right) \tag{10}$$

$$L_{12} \approx \frac{K_{12}}{2\pi f_0}, \qquad (\text{for } K_{12} \ll Z_0). \tag{11}$$

3) Admittance Inverter:

$$B_{23} = \frac{J_{23}}{1 - (J_{23}Z_0)^2} \tag{12}$$

$$l_{23} = \frac{\lambda}{4\pi} \tan^{-1}(2B_{23}Z_0) \tag{13}$$

where λ is the wavelength of the transmission line at f_0.

The synthesis for an X-band amplifier with

$$f = 8.0\text{–}12.0 \text{ GHz}$$
$$R_{im} = 21\ \Omega$$
$$C_{im} = 0.57 \text{ pF}$$
$$Z_0 = 50\ \Omega$$

yields the network that is shown in Fig. 7. The resulting computed source admittance Y_s at the MESFET input deviates most from the target Y_{sm} at 12 GHz. At this frequency, it raises the noise figure 0.2 dB[3] above the design objective shown in Fig. 2. Computer optimizing this circuit results in the element values shown in parentheses in Fig. 7. Only small changes are necessary to achieve optimum performance. The microstrip realization illustrated in Fig. 8 shows that all network elements are easily realized. The two inductances are approximated with short bonding wires and the series capacitance by a narrow gap between the ends of adjacent transmission lines. The shunt inductance facilitates gate bias insertion, and the series capacitance acts as a dc block. Below the passband, the shorted shunt line and the series capacitance form a high-pass filter at the amplifier input. This structure reflects low frequency signals and protects the Schottky-barrier gate from burnout.

B. Output Coupling Network

In general, an amplifier is required to have low output VSWR and constant power gain in the design band. However, the available power gain of the MESFET, when matched for minimum noise measure, exhibits a slope of approximately 4.7 dB/octave (Fig. 2). Therefore, an ideal output network has to couple all available power to the load at the upper band edge f_u and provide a frequency dependent attenuation that compensates the FET's gain slope for $f < f_u$.

A simple network suitable for this purpose is shown in Fig. 9. The output admittance of the transistor, R_{om} in parallel with C_{om}, is resonated with the series inductance L_o at f_u. The transformer matches the resulting resistance to the load Z_0. At f_u, no power is dissipated in the resistor R_1 since it is connected in series with a short-circuited shunt stub that is a quarter-wave long at this frequency. Below f_u, the power transferred to the load decreases because the impedance of the resonated FET output

[3] This excess noise figure was computed with formula 1 of [11]. The four noise parameters were determined from data presented in Figs. 2 and 3.

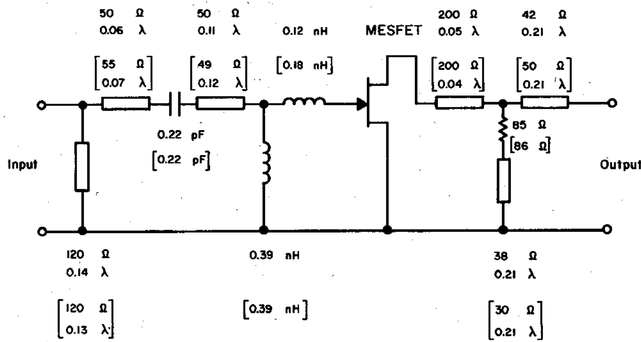

Fig. 7. Single-stage X-band amplifier circuit. Element values calculated with the formulas and curves of Section III are compared with computer optimized values (in parentheses). The transmission lines are defined by their characteristic impedances and lengths which are expressed as fractions of a wavelength at 10 GHz.

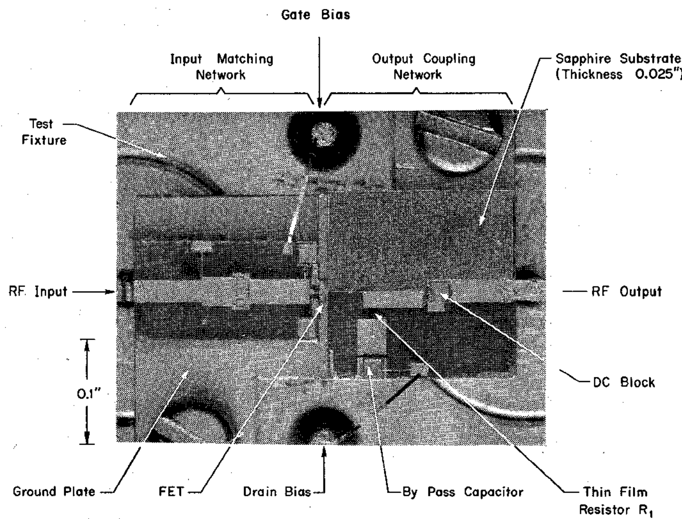

Fig. 8. Realization of the single-stage X-band amplifier.

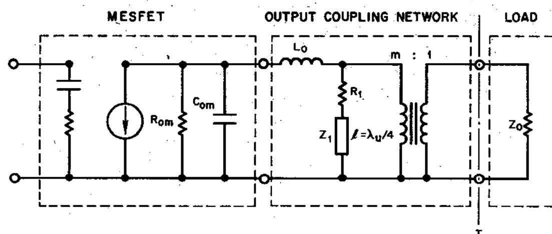

Fig. 9. MESFET with output coupling network.

changes rapidly and the shunt branch with the resistor becomes increasingly lossy.

The resistance R_1 and the characteristic impedance of the transmission line Z_1 were varied until the best approximation to a 4.7-dB/octave slope for the output circuit transducer loss was obtained. Fig. 10 shows the results optimized for a frequency range of $f_u/f_l = 1.5{:}1$ with the MESFET output Q

$$Q = 2\pi f_u R_{om} C_{om} \tag{14}$$

as a variable. It is seen that this simple network is useful as long as Q does not exceed 2.5. Under this condition, the maximum deviation from the 4.7-dB/octave transducer

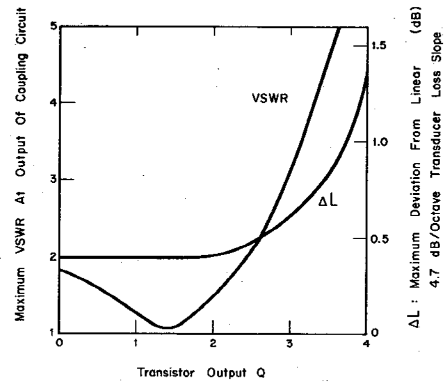

Fig. 10. Transducer loss and VSWR (in plane T) of output coupling circuit versus transistor output Q. For each Q value, the circuit has been optimized to yield a perfect power match at the upper band edge and exhibit a 4.7-dB/octave slope in transducer loss within the $f_u/f_l = 1.5{:}1$ frequency range.

loss target is less than 0.5 dB and the output VSWR does not exceed 2:1. For higher Q values, a more complex circuit is required to shape the coupling loss versus frequency curve and keep the output match within acceptable limits. The optimum element values are plotted in Fig. 11. Using these curves, the X-band circuit, as shown in Fig. 7, has been designed for

$$R_{om} = 192\ \Omega$$
$$C_{om} = 0.16\ \text{pF}$$
$$f_u = 12\ \text{GHz}$$

which yields a Q of 2.3. The inductance is too large (0.9 nH) to be realized in lumped form and is modeled as a short high-impedance transmission line. It consists of a bonding wire which runs parallel to and above the ground plane. At the output, the ideal transformer is approximated with a 42-Ω $\lambda/4$ transmission line, which is sufficiently broad band for this case. The accuracy of this design for the exact MESFET model with bilateral characteristics has been evaluated. For this purpose, the output circuit has been computer optimized with the MESFET represented by its s parameters and with the input circuit of Fig. 7 (values

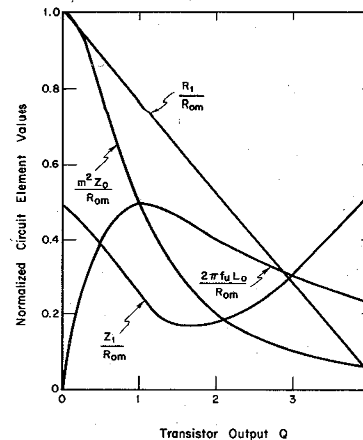

Fig. 11. Optimum values for circuit elements of the output coupling network versus transistor output Q.

stated in parentheses) connected. The resulting element values are shown in parentheses in Fig. 7. They are very close to the values obtained from Fig. 11. The microstrip realization is illustrated in Fig. 8.

C. Amplifier Construction

The basic building block is a single-stage amplifier which is approximately matched to a 50-Ω source and load and uses the circuits described in the previous sections. Such an amplifier unit is shown in Fig. 8. The circuits with resistors, interdigitated capacitors, and transmission lines are fabricated on 0.025-in sapphire substrates. The substrates are soldered onto a ground plate and are separated by a ridge on which the transistor chip is mounted. In this configuration, the transistor source can be grounded with less than 50-pH lead inductance, and RF power leakage from the FET output to input is minimized. RF bypass and dc blocking capacitors are soldered onto the substrates, and the devices are interconnected with thermocompression bonded gold wires. After assembly, the single-stage units are mounted in a test fixture where they are tuned and characterized.

For the X-band amplifier, three identical single-stage units were cascaded. This modular approach does not achieve the widest possible bandwidth, but it has the following practical advantages.

1) The design and fabrication are limited to two circuits.

2) The tuning of a few variables on a single-stage amplifier is efficient and convergent.

3) In final assembly, stages can be selected according to their tuned performance (e.g., lowest noise unit selected for first stage).

4) In the case of device failure, each stage can be easily exchanged with only minor retuning of the amplifier.

The assembled stages are built into a metallic enclosure that acts as a waveguide below cutoff, thus suppressing modes that cause resonances and RF leakage from output to input.

IV. X-BAND AMPLIFIER PERFORMANCE

The gain and noise figures of the three-stage amplifier are plotted versus frequency in Fig. 12. From 8.0 to 12.0 GHz, the power gain is 20.7 dB with less than ±1.3-dB variation. A single stage yields a constant gain of 7 dB up to 12 GHz. This is only 0.6 dB less than the maximum possible gain predicted on the basis of the measured device gain (Fig. 2) under the operating conditions for minimum noise measure. The gain variation is close to the minimum value of 1.2 dB that can be achieved with the simple output circuit (Fig. 10). The reverse insertion loss $|s_{12}|^{-2}$ does not drop below 50 dB (Fig. 13) which indicates that for high-gain requirements more than three stages can be cascaded without loss of stability. The maximum local gain slope is 0.005 dB/MHz, and the gain dependence on ambient temperature under constant bias conditions is −0.07 dB/°C. Improved stability can be obtained with a temperature-controlled gate bias circuit. The transmission

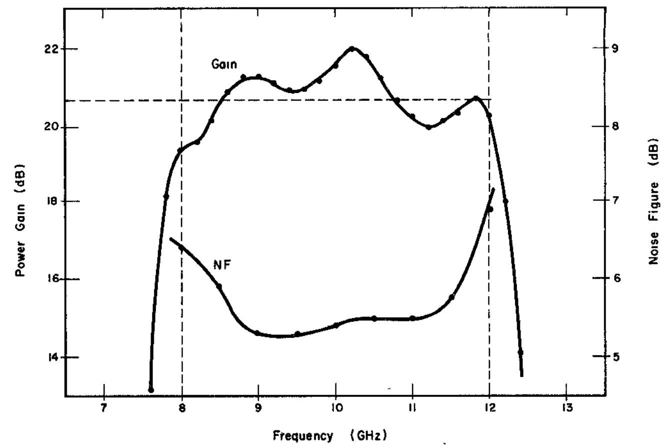

Fig. 12. Power gain and noise figure versus frequency for the three-stage X-band amplifier.

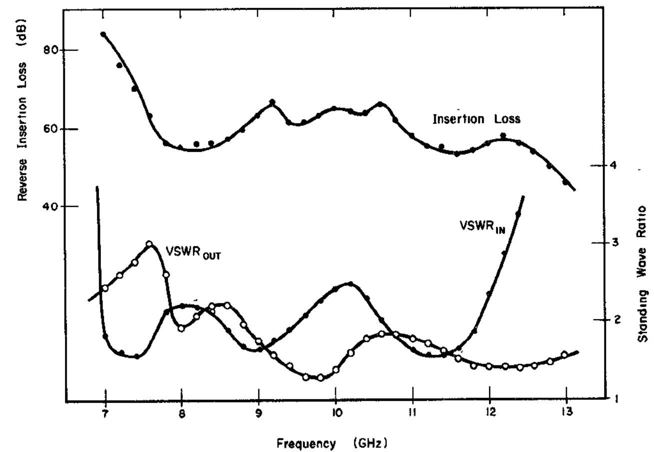

Fig. 13. Input and output VSWR and reverse insertion loss versus frequency for the three-stage X-band amplifier.

phase deviation from linearity is less than ±14° between 8 and 12 GHz.

The most noteworthy characteristic of this amplifier is the low noise figure which does not exceed 5.9 dB over the wide range of 8.5–11.5 GHz. At 10 GHz, for example, the first stage has a noise figure of 4.6 dB with 7.0-dB gain. The transistor used in this stage, which is biased for minimum noise measure, exhibits a noise figure of 3.9 dB with 9.0-dB associated (device) gain. The 0.7-dB difference in noise figure is caused by attenuation in the coaxial to microstrip transition, attenuation in the input network (approximately 0.3 dB), and by a mismatch with respect to the optimum admittance for lowest noise measure. The contributions from the following stages raise the overall amplifier noise figure to 5.4 dB. At the lower and upper band edge, the noise match of the input stage degrades, which causes the noise figure to increase. At 12 GHz, the maximum value of 6.9 dB is reached. In comparison, a narrow-band design that was optimized at 8 GHz yielded a minimum noise figure of 3.9 dB with 25-dB gain. The lowest possible amplifier noise figure, as determined from Fig. 2 (curve ④), is 3.6 dB at this frequency. At the edges of an 800-MHz band, the noise figure degrades to 4.4 dB.

These narrow-band amplifier data are similar to results reported in [9].

The standing wave ratios at the input and output ports are shown in Fig. 13. The input VSWR does not exceed 2.4:1 even though the circuit is designed for a noise match as opposed to an impedance match. This performance clearly demonstrates the broad-band matching capability of this input network. The output VSWR is 1.4:1 at 12 GHz and 2:1 at 8 GHz. The simple output coupling circuit provides a good impedance match at 12 GHz and is capable of attenuating the excess power at lower frequencies rather than reflecting it. This characteristic is essential for the success of the modular approach in which pretuned stages are cascaded.

The large signal properties of the three-stage amplifier are also noteworthy. In order to increase the dynamic range, the drain current of the MESFET in the output stage was raised to 50 mA. The drain voltage was left unchanged at 4 V. The minimum output power for 1-dB gain compression is +13 dBm reached at 10 GHz. At this frequency, the third-order intermodulation intercept is +26 dBm. In a different circuit specially designed for a power output stage, +20-dBm output power at 5-dB gain[4] was obtained with a single transistor. The MESFET, biased at 6-V drain voltage and 43-mA drain current, exhibited a drain-efficiency ($P_{\text{RF-out}}/P_{\text{dc-in}}$) of 39 percent.

To determine the nuclear radiation hardness of the amplifier, packaged MESFET's have been subjected to the fast neutron radiation of an unmoderated pulsed uranium reactor.[5] A flux of 5×10^{14} neutrons/cm^2 yields a 10-percent decrease in transconductance. A ten times higher neutron fluence causes extensive lattice damage (traps) such that most free carriers are removed, and the drain current drops to zero. Results published for GaAs JFET's with the same channel doping and of similar structure [13] show the same parameter degradation at an order of magnitude higher neutron fluence. The results, however, are difficult to compare because in [13] a moderated reactor with a spectrum rich in low energetic neutrons was used. The MESFET's were also subjected to the 1.25-MeV gamma radiation of a cobalt-60 source. Absorbed doses up to 10^8 rad (GaAs) caused no detectable change in transconductance.

V. CONCLUSIONS

Optimum low-noise amplifier performance is obtained with MESFET's biased for minimum noise measure and with an input coupling network designed to synthesize the optimum source admittance for lowest noise measure. The input circuit consists of a series inductance and quarter-wave resonators alternately coupled by impedance and admittance inverters. The network design is based on Chebyshev impedance-matching prototypes. A series inductance and a transformer match the MESFET's output admittance to the load at the upper band edge. A lossy shunt stub provides frequency dependent attenuation compensating the MESFET's gain slope. Optimized design curves are presented for this output coupling network. The circuits yield amplifier stages that are stable, approximately matched to 50 Ω, and easy to realize in microstrip.

An 8.0–12.0-GHz amplifier was built with three identical cascaded stages. The amplifier exhibits a maximum noise figure of 6.9 dB (5.5 dB typical) with 20.7 ± 1.3-dB gain. The VSWR at the input and output ports does not exceed 2.5:1. The minimum output power for 1-dB gain compression is +13 dBm, and the intercept point for third-order intermodulation products is +26 dBm.

These experimental results demonstrate that amplifiers with GaAs MESFET's can be designed to yield high-gain and low-noise properties over wide bandwidths. In this frequency range (>8 GHz), bipolar transistors have insufficient gain for low-noise amplifiers ($G \leq 4$ dB with 4-dB noise figure at 8 GHz), and tunnel diodes exhibit very limited dynamic range (IM intercept point < -10 dBm). For ultra-low-noise receiver requirements ($NF \leq 3$ dB), parametric amplifiers still hold a unique position. However, if the parametric amplifier is excluded because of its complexity and cost, then the MESFET is presently the only solid-state device suitable for low-noise amplification in X and Ku bands with acceptable dynamic range. The data reported in this paper confirm that MESFET amplifiers meet specifications that are equivalent to those imposed on low-noise traveling wave tube amplifiers. The MESFET amplifier qualifies, therefore, as the solid-state replacement in this frequency range.

[4] The small-signal gain was 7.5 dB at 10 GHz.

[5] Reactor SPR II of Sandia Laboratories, Albuquerque, New Mex.

ACKNOWLEDGMENT

The authors wish to thank R. Larrick for his measurement assistance and valuable experimental contributions, Dr. J. Barrera and R. Drabin for supplying the GaAs epitaxial layers, E. Gowen for the MESFET fabrication, D. Hollars for the microcircuit assembly, and Dr. E. Graham of Sandia Laboratories for the neutron and gamma irradiation experiments. They also wish to thank Dr. R. Archer, A. Podell, R. Van Tuyl, J. Dupre, and J. Kesperis for helpful suggestions and comments.

REFERENCES

[1] W. Baechtold *et al.*, "Si and GaAs 0.5μm-gate Schottky-barrier field-effect transistors," *Electron. Lett.*, vol. 9, pp. 232–234, May 1973.

[2] C. A. Liechti, E. Gowen, and J. Cohen, "GaAs microwave Schottky-gate field-effect transistor," in *ISSCC Dig. Tech. Papers*, 1972, pp. 158–159.

[3] N. G. Bechtel, W. W. Hooper, and D. Mock, "X-band GaAs FET," *Microwave J.*, vol. 15, pp. 15–19, Nov. 1972.

[4] P. L. Clouser, and V. V. Risser, "C-band FET amplifiers," in *ISSCC Dig. Tech. Papers*, 1970, pp. 52–53.

[5] W. Baechtold, "Ku-band GaAs FET amplifier and oscillator," *Electron. Lett.*, vol. 7, pp. 275–276, May 1971.

[6] S. Arnold, "Single and dual gate FET integrated amplifiers in C-band," in *IEEE Int. Microwave Symp. Dig. Tech. Papers*, 1972, pp. 233–234.

[7] L. Besser, "Design considerations of a 3.1–3.5 GHz GaAs FET feedback amplifier," in *IEEE Int. Microwave Symp. Dig. Tech. Papers*, 1972, pp. 230–232.

[8] R. Zuleeg, E. W. Bledl, and A. F. Behle, "Broadband GaAs field effect transistor amplifier," Air Force Avionics Lab.,

Wright-Patterson Air Force Base, Ohio, Tech. Rep. AFAL-TR-73-109, Mar. 1973.

[9] W. Baechtold, "*X*- and *Ku*-band amplifiers with GaAs Schottky-barrier field-effect transistors," *IEEE J. Solid-State Circuits* (*Special Issue on Microwave Integrated Circuits*), vol. SC-8, pp. 54–58, Feb. 1973.

[10] C. A. Liechti and R. L. Tillman, "Application of GaAs Schottky-barrier FETs in microwave amplifiers," in *ISSCC Dig. Tech. Papers*, 1973, pp. 74–75.

[11] H. Fukui, "Available power gain, noise figure, and noise measure of two-ports and their graphical representations," *IEEE Trans. Circuit Theory*, vol. CT-3, pp. 137–142, June 1966.

[12] G. L. Matthaei, L. Young, and E. M. T. Jones, *Microwave Filters, Impedance-Matching Networks, and Coupling Structures*. New York: McGraw-Hill, 1964.

[13] A. F. Behle and R. Zuleeg, "Fast neutron tolerance of GaAs JFET's operating in the hot electron range," *IEEE Trans. Electron Devices* (Corresp.), vol. ED-19, pp. 993–995, Aug. 1972.

AM and FM Noise of BARITT Oscillators

JOSEF L. FIKART, MEMBER, IEEE

***Abstract*—AM, FM, and baseband noise of a BARITT diode oscillator in the range 100 Hz–50 kHz off the carrier has been measured under various operating conditions. A simple calculation has been made, relating the baseband noise to the oscillator AM and FM noise via measured amplitude and frequency modulation sensitivities and the results have been compared with the noise measured. It is shown that, depending on the bias current applied, both AM and FM noise performance can be degraded by up-conversion. Complete removal of up-converted noise requires a high-impedance low-noise bias supply since both the diode noise and bias supply noise at baseband frequencies may be significant when up-converted. Even with all modulation suppressed, the AM and FM noise has a flicker component almost completely correlated with the diode flicker noise at baseband frequencies. The RF power dependence of the AM and FM noise has also been investigated. It is shown that the BARITT oscillator noise compares very favorably with that of IMPATT's and TEO's. Values of −142 dB/100 Hz (AM noise) and 3.5 Hz/(100 Hz)$^{1/2}$ for $Q_{ext}=200$ (FM noise) have been measured at 30 kHz off the carrier.**

I. INTRODUCTION

With their capability of producing low-noise microwave power in moderate amounts, BARITT diodes have become potential contenders to TEO's in local oscillator applications. Several theoretical studies of small-signal noise in BARITT's were carried out [1]–[3] and the principal noise sources (except for flicker noise) seem to have been identified. The results were given in terms of the small-signal noise measure. No theoretical large-signal noise analysis has been presented so far; perhaps the theories in [4],[5] or [6],[7], originally conceived for IMPATT's, could be used for this purpose once a suitable large-signal deterministic analysis is available for the BARITT diode. The experimental data on noise measure [8]–[11] indicate relatively small differences (10 dB on the average) between the small-signal and large-signal noise measures of BARRITT diodes.

However, there still is a considerable lack of information on the behavior of BARITT oscillator AM and FM noise, rather than noise measure, under various operating conditions. One reason for investigating AM and FM noise directly is the fact that the large-signal noise measure transforms differently into them [5],[6]; one can introduce the concept of AM and FM noise measure [5]. Another factor is the modulation noise which can sometimes completely mask the so-called "primary" noise, i.e., the internal noise generated by the device in the band about the center frequency. An effort in this direction was made by Herbst and Harth [11],[12] who measured the frequency modulation sensitivity of a Pd-n-p$^+$ BARITT diode in dependence on modulation frequency and bias current, in conjunction with FM noise measurements.

It is the purpose of this work to find out, by means of simple calculation and experiment, how both the total AM and FM noise are influenced by modulation noise, bias impedance levels, RF power level, etc., and to determine what minimum AM and FM noise can be expected and under what conditions. We will also be interested in seeing how the BARITT noise compares with that of other solid-state microwave generators.

II. CONDENSED THEORY

From the simple equivalent oscillator circuit in Fig. 1, and using well-known formulas for the primary noise deduced from [13],[14], the following relations can be written for AM and FM noise, respectively, while neglecting cross correlation between "primary" and modu-

Manuscript received August 24, 1973; revised December 20, 1973. This work was supported by the National Research Council of Canada, under the terms of a postdoctoral fellowship.

The author was with the Department of Electrical Engineering, the University of Alberta, Edmonton, Alta., Canada. He is now with GTE Lenkurt (Canada) Ltd., Burnaby, B. C., Canada.